Frontiers in Scientific Research and Technology

Online ISSN: 2682-2970
Print ISSN: 2682-2962
http://fsrt.journals.ekb.eg

FSRT J 7 (2023) 21 - 34 10.21608/FSRT.2023.224935.1099

Petrography, mineralogy, and fluid inclusions of Rod El-Biram muscovite pegmatites, Central Eastern Desert, Egypt.

Waheed Elwan[1*], Ahmed M. Dardir[2], Emad Khalil[1], Mohamed Abdelmoniem Mohamed[3], Hader Sobhy[1], and Fares Khedr[4]

[1]Geology Department, Faculty of Science, Zagazig University, Zagazig-44519, Egypt.
[2] Nuclear Material Authority, Maadi, Cairo, Egypt.
[3] Faculty of Science, Assiut University, Assiute-71516 Egypt
[4]Geology Department, Faculty of Science, Suez University, Suez, Egypt.

ARTICLE INFO

Article history:
Received 25 July 2023
Received in revised form 16 August 2023
Accepted 23 August 2023
Available online 27 August 2023

Keywords
Pegmatite,
Eastern Desert,
Fluid inclusions,
Wadi Rod El-Biram,
Heavy minerals.

ABSTRACT

Wadi Rod El-Biram pegmatites muscovite pegmatite are located at the Central Eastern Desert between latitudes 25º 8` 30`` and 25º 11` N and longitudes 34º and 34º 10`E. They occur as rounded or elongated zoned masses and they invade both alkali-feldspar granites and ophiolitic serpentinites. The zoned bodies consist of a) wall zone, which composed mainly of albite and muscovite. Greisenized pockets are extending between alkali-feldspar granites and the wall zone, b) the intermediate zone, which consists mainly of K-feldspar with subordinate amount of quartz and muscovite and c) the core zone, which consists mainly of amoeboid-shaped milky quartz and may enclose isolated flakes and/or nests of muscovite. The heavy minerals contain garnet, fluorite, zircon, and rutile minerals. Garnet may be derived either by crystallization with muscovite as an alternative to biotite from volatile enriched melt or by assimilation from country rocks. Fluid inclusions are represented by coexisting of two-phase and three-phase inclusions. The estimated conditions of trapping using the intersection of isochors are at temperature range between (360-420 ºC), and pressure between (600-2100 bars). Rod El-Biram muscovites have primary magmatic origin. The trend of the granitic rock and the associated pegmatites in Rod El-Biram is not compatible with the fractional crystallization, so the pegmatites have a different source rather than the granitic melt. These S-type pegmatites may have originated by partial melting of a metasedimentary source. The chemical composition K-feldspars and physical testing confirms the suitability of the feldspars from Rod El-Biram pegmatites for floor rather than wall ceramic tiles.

1. Introduction

Pegmatites are defined by textural attributes rather than by composition. The coarse size of crystals is a hallmark of many pegmatites. Pegmatite bodies vary greatly in size and shape; their shapes vary from pockets, dykes, sheets to huge plugs. Pegmatites are one of the main sources of metals like, Nb, Ta, Sn, Zr, Y, Be, B, Li, Cs, Bi and REEs, and semi-precious gemstones such as topaz, beryl and tourmaline (Černý et al., 2012). In addition, they also represent the main sources of feldspar, which is used in the ceramics, glass and electronics industries. Pegmatites in a particular field may show a regional mineralogical-chemical zonation (Černy, 1982). Most pegmatites possess the composition of granite but pegmatites of basic, intermediate, or alkaline composition are also common. Rudenko et al. (1975) classified pegmatites into ceramic, mica-bearing, rare-metal bearing, and rock-crystal bearing.

Ginsburg (1984) established a classification scheme for the formations of pegmatites based on their mineralogical or textural features and related to depth of emplacement, which include abyssal, muscovite, rare-element, and miarolitic. Černy (1991) classified pegmatites into a) abyssal classes, which were formed under high to low pressure, b) muscovite classes, which commonly formed at high pressure and low temperature, c) rare element classes, which were formed at low temperature and pressure, and d) miarolitic or shallow level pegmatites. The rare-element classes are subdivided based on their composition into LCT and NYF types: LCT are Li, Cs, and Ta- rich, whereas NYF are Nb, Y, and F- rich. Wise (1999) related the NYF pegmatites to A-type granite plutons, while LCT pegmatites are related to post-tectonic to anorogenic plutons. Černy & Ercit (2005) classified pegmatites into three petrogenetic families, which are: NYF family, a peraluminous LCT family and a mixed NYF + LCT family. Martin and De Vito (2005) suggested that LCT pegmatites are generated in compressional or orogenic tectonic settings, while NYF formed in extensional or anorogenic tectonic settings. On the other hand, mixed NYF and LCT

* Corresponding author at Zagazig University

E-mail addresses: wielwan@science.zu.edu.eg (Waheed Elwan)

pegmatites could be generated as a result of contamination, either at the magmatic or post-magmatic stage. The mixed LCT + NYF family designates pegmatites that show composite properties of the two other families. The mixing of magma from different sources or metasomatic overprint by late melt or fluid might explain the geochemical features of mixed LCT + NYF pegmatites (Martin and De Vito, 2005; Müller et al., 2017).

1.1. Internal structure of pegmatite

Cameron et al. (1949) described three lithologic and structural units found in many pegmatites. These include a) zones or successive shells, which are complete or incomplete, reflecting variation in the shape and structure of the pegmatite body, b) fractures filling the previously consolidated pegmatite and c) replacement bodies, which are formed primarily by replacement of pre-existing pegmatite, with or without obvious structural control. The zones have been divided in the following manner from the margin to the center: border zone, wall zone, intermediate zone, and core.

Four pegmatites field can be recognized in the Eastern Desert of Egypt (Rashwan, 1991; Khaleal et al., 2022) namely: a) Gattar- Wadi Hebal pegmatite field that located at the northern portion of Eastern Desert (Shalaby et al., 1999; El-Nahas, 1997), b) Wadi Bezah pegmatite field, which located at the central portion of the Eastern Desert, c) Migif-Hafafit pegmatite field that lies between the central and southern parts of Eastern Desert and d) Umm Rasein-Hamaany pegmatite field, which located at Southern portion of the Eastern Desert. Many LCT and NYF pegmatite localities have been recorded in Eastern Desert of Egypt. For example, LCT-pegmatites in Abu Rusheid (Raslan & Ali, 2011; Ibrahim et al., 2017), whereas NYF-pegmatites occur at Kadabora (Saleh, 2007), Ras Baroud (Raslan et al., 2010a; Fawzy et al., 2020), Wadi Khuda (Raslan et al., 2010b), Abu Rusheid (Raslan & Ali 2011), and Gabal El Faliq (Abu Elatta, 2019). However, the mixed LCT-NYF pegmatites in Egypt still need to be properly described, in order to assess their genesis and their economic potential. Rare metal and radioactive granitic pegmatites were reported in many areas of the Egyptian Eastern Desert (e.g., Omar, 1995; Raslan et al., 2010a; Saleh et al., 2019).

Most pegmatites are granitic in composition, and they are cogenetic with the associated granites. Barren pegmatites are widely scattered and distributed, as veins or dykes in different country rocks at various areas all over the Egyptian Eastern Desert (Fawzy et al., 2020), whereas the mineralized zoned pegmatite bodies are rare. Pegmatites are widely distributed in the northern portion of Egyptian Eastern Desert. They vary in length, width, and direction. They are penetrated and/or invaded migmatite-gneiss, gneiss, granodiorite, tonalite, trondhjemite and alkali granites.

Dardier (1997) described the pegmatites at Wadi Rod El-Biram as small pockets and lenses that enclosed within low hilly granitoids along Wadi Rod El-Biram; their quartz core is generally of milky white color, with iron staining.

Moustafa et al. (2002) distinguished three successive zones in the pegmatites of Wadi Rod El-Biram which are, a) The wall zone b) the intermediate zone and c) the core. They suggested that Rod El-Biram pegmatites were derived by fractional crystallization melt generating by partial melting of the enclosing rocks. These pegmatites were considered as complex zoned pegmatites by El-Shibiny (2016).

The present work focuses on the study the detailed petrographical, mineralogical, fluid inclusion, mineral chemistry, and physical testing characterization of Rod El-Biram zoned muscovite pegmatites aiming to shed more light on Rod El-Biram pegmatite body mode of formation and their suitability for ceramic industry.

2. Analytical techniques

The heavy minerals from Wadi Rod El-Biram pegmatite body and the Scanning Electron Microscope (SEM) investigation of separated minerals were carried out at the laboratories of Nuclear Material Authority. For the mineralogical investigations, the heavy liquids separation technique using bromoform and magnetic fractionation using a Frantz Isodynamic Magnetic Separator, then each fraction subjected to hand picking under binocular stereomicroscope. The mineralogical investigation was carried out using SEM model (PHILIPS XL 30) attached with Energy Dispersive X-ray unit (EDX). The microanalyzer worked out at an operating voltage of 25 KV, 1-2mm diameter, 60-120 second counting time and high-resolution backscattered electron images (BSE) with using ZAF correction errors. The fluid inclusion petrography and microthermometric measurements were carried out on 3 doubly polished wafers quartz samples 0.2-0.3 mm thick using a Chaixmeca heating freezing stage (Poty et al., 1976) at Geology Department, Assiute University. The stage was calibrated for temperatures between -100 and 400℃ using Merck chemical standards as well as according to the melting point of distilled water (0 ℃) and phase transition in natural pure CO_2 inclusions with triple point (56.6 ℃). From microthermometric results the bulk composition and density of the fluids could be calculated by using the equation of state of Zang & Frantz (1987) for the H_2O- NaCl system, and Bowers & Helgeson (1983) for volatile rich system. Isochores for different fluid densities are calculated until a fit with the known homogenization temperature is achieved using the Flincor computer program (Brown, 1998). The minimum pressure of trapping is estimated from the constructed P-T diagramsThe chemical analyses of, granitic samples, separated muscovite, K-feldspar, wall zones and border zones from the pegmatite body were carried out using X-Ray Fluorescence Analyses for major elements using Phillips Origaku 3070 with eight analyzing crystals and maximum power of the equipment was 30 K.wt., Crystals (LIF-200), (LIF-220) at Central Laboratories of Mineral Resources Authority, Cairo, Egypt. The physical parameters tests on the prepared green biscuit samples from intermediate zone. The prepared green ceramic samples are 5 cm in width and 10 cm in length with 1.52 cm thickness. They pressed using SACMI imola presser. Each green ceramic

sample was dried and fired, then shrinkage testing was carried out using Vernier caliper 150 x 0.05 mm. Shrinkage is the rate of change in length and width for inspection sample. Samples were subjected to stress testing for measuring the bending stress by using Gabbrielli Crometro CR5 instrument. Finally, the water absorption was measured for each sample. These tests were carried out in the Laboratories of Arab Contractors Company.

3. Geologic background

Rod El-Biram pegmatite bodies are outcrops in the Central Eastern Desert at the latitude 25º 8` 30`` and 25º 11` 00`` N and longitude 34º 00` 00`` and 34º 10` 00`` E north Idfu-Marsa Allam asphaltic Road (Fig.1a & b). Their elevation ranges from 497 to 524 meters above sea level. The main rock units exposed in the studied area are represented by ophiolitic serpentinites, arc metavolcanics, older granites, intrusive younger gabbros, younger granites and pegmatites. Rod El-Biram pegmatite bodies invade both of younger granites and ophiolitic serpentinites. Host-rock inclusions in pegmatites are rare except for thin bands of talc-chlorite along their contacts.

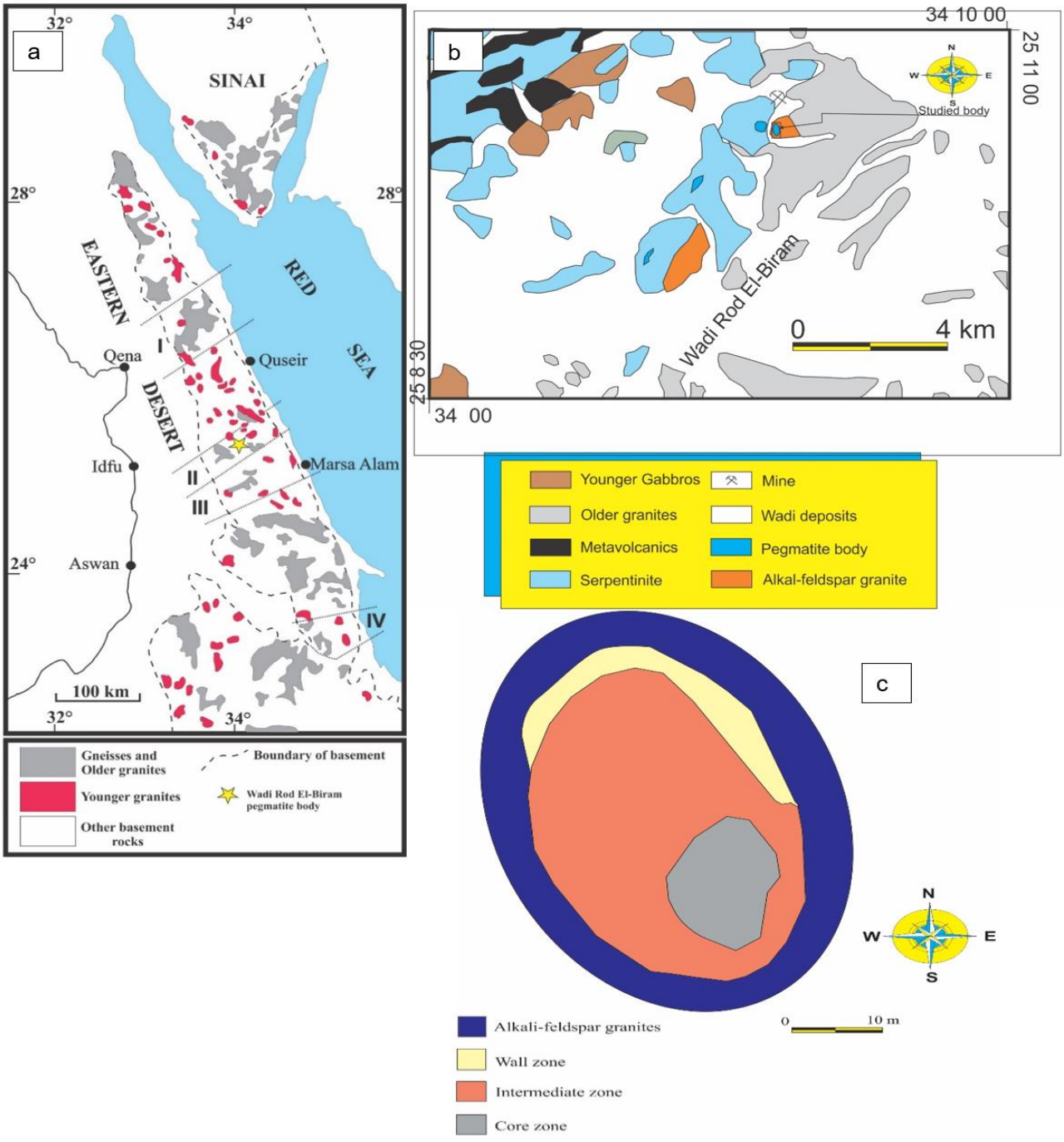

Fig.1: a) location map of Rod El-Biram pegmatite body, I; II; III Northern Eastern Desert, Central Easter Desert and Southern Eastern Desert respectively; b) Geologic map of Wadi Rod El-Biram area (modified after El-Shibiny, 2016); c) Sketch of zoned pegmatite body of Wadi Rod El-Biram area.

The ophiolitic serpentinite occurs as isolated irregular hills associated with talc-carbonate rocks. The ophiolitic serpentinite mass varies in color from brown to reddish brown color.

The younger granites are represented by alkali-feldspar granites, reveal grayish-white color. They intrude the ophiolitic serpentinite and older granites with sharp intrusive contacts.

Road El-Biram pegmatites are a member of a Wadi Bezah pegmatite field along Idfu-Mersa Alam Road. The pegmatite bodies are classified to muscovite-bearing type, which occur in the form of round and elongated masses (Fig.1b). The main pegmatite bodies vary in thickness from 60 to 100 m and striking in WNW-ESE with gently dip 200 to NNE. Doleritic dyke (1-5 cm thick with E-W direction) invades pegmatite bodies. The pegmatite bodies of Wadi Rod El-Biram are varied from zoned to unzoned. The zoned bodies consist of three zones: the outer, the intermediate and the inner zones (Fig.2 a- d).

Generally, the grain size increases gradually from the wall zone through the intermediate zone to the core zone. The outer zone (wall zone) is composed mainly of albite and muscovite. Greisenized pockets are recorded along contact between alkali-feldspar granites and the wall zone of pegmatite body (Fig.2b).

The intermediate zone consists mainly of blocky K-feldspar (Fig.2c) i.e., microcline and orthoclase in a decreasing order of abundance (Plate 1a & b). This zone represents the main constituent of the pegmatite body and contains subordinate amounts of quartz and muscovite (Plate1c). The color of K-feldspars sometimes changed into brick-red due to ferrugination (Plate 1b).

The inner zone (core zone**)** is mainly made up of milky quartz (Plate 1d; Fig.2c), forming an amoeboid shape. Sometimes, quartz core encloses isolated flakes and/or nests of muscovite (Plate1e; Fig.2d) and rarely biotite and opaques. Large euhedral six-sided quartz crystals are recorded within the core zone.

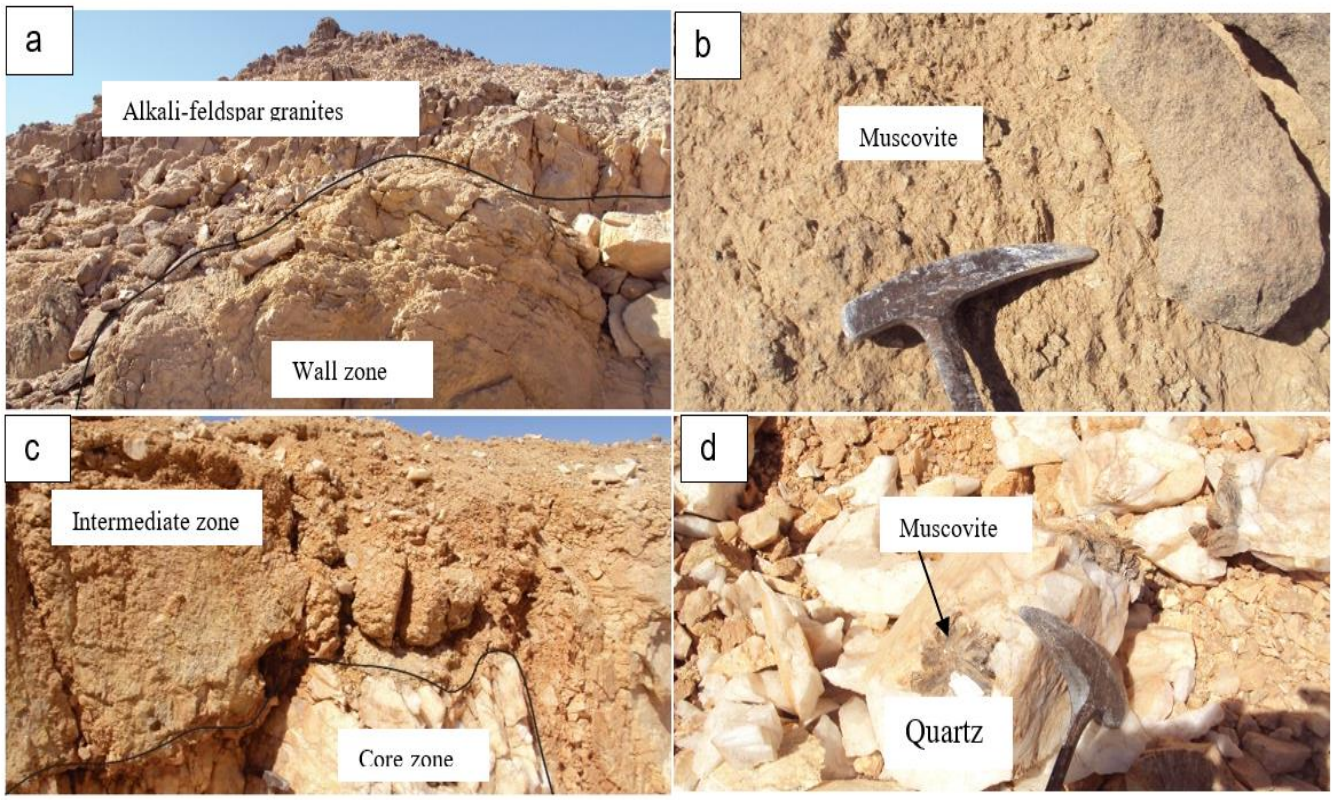

Fig.2.: Contact between alkali-feldspar granites and wall zone, Wadi Rod El-Biram area; b) Fan-shaped muscovite (greisenized pockets) along contact between alkali-feldspar granites and wall zone; c) Contact between intermediate zone and core Zone; d) Quartz with rosette-shape mica nests in core zone.

4. Petrography

4.1. Alkali-feldspar granites

They are medium-grained rocks show greyish color with hypidiomorphic texture. They are essentially composed of K-feldspar, plagioclase, and quartz. Kaolinite, sericite, and muscovite are found as secondary minerals, while the accessory minerals are muscovite, garnet, iron oxides, zircon and apatite.

K-feldspar occurs as subhedral phenocrysts of patchy-type perthite and in some parts reveal partially altered to sericite and kaolinite. Plagioclase occurs as subhedral lamellar crystals characterized by albite and pericline twinning. Some plagioclase crystals are microfolded (Fig.3a) and cracked indicating effects of deformation phase. These cracks are filled with hematite or secondary muscovite. Quartz occurs as subhedral phenocrysts, which corrodes both K-feldspar and plagioclase. Muscovite

occurs as primary, secondary after feldspar or fracture filling. Primary muscovite occurs as subhedral flakes. Garnet occurs as subhedral crystals distinguished by their high relief (Fig.3b). It is partially altered to muscovite along their internal cracks. Iron oxides are represented by ilmenite and magnetite. Zircon occurs either as subhedral crystal enclosed within quartz or within feldspar or as small, rounded grains. Some crystals show pleochroic halos. Apatite occurs as small needles enclosed within garnet.

4.2. Zoned pegmatites

The zoned pegmatite bodies are composed of three successive zones, which are: a) wall zone is mainly composed of albite and muscovite. Albite (5-10) forms subhedral cracked crystals showing albite twinning. These cracks are filled with hematite and sericite. Muscovite occurs as irregular elongated flakes. Greisenized pockets are recorded along the contact between alkali-feldspar granites and the wall zone (Fig.3c), b) intermediate zone mainly consists of blocky K-feldspar with or without muscovite. Fluorite and garnet are rare as accessory minerals.

K-feldspar occurs as microcline and microcline perthite. Perthites in this zone show vein, string, and flame- type perthites (Fig.3d). Muscovite is partially altered to chlorite and gradually increases from wall zone towards intermediate zone. It forms large clots of radiated crystals forming variolitic and fan shape textures (Fig.3e). Garnet occurs as subhedral grains, which are partially or completely altered to muscovite. Fluorite occurs as small isotropic crystals and it is commonly associated with muscovite (Fig.3f). Apatite occurs as long prismatic or needle-like crystals, while monazite occurs as fine anhedral grains, c) core zone is mainly composed mainly of quartz. Quartz forms interstitial anhedral crystals, corroding mica and K-feldspars. The cracks within quartz are usually filled with epidote, clay minerals and iron oxy-hydroxides forming net-like texture.

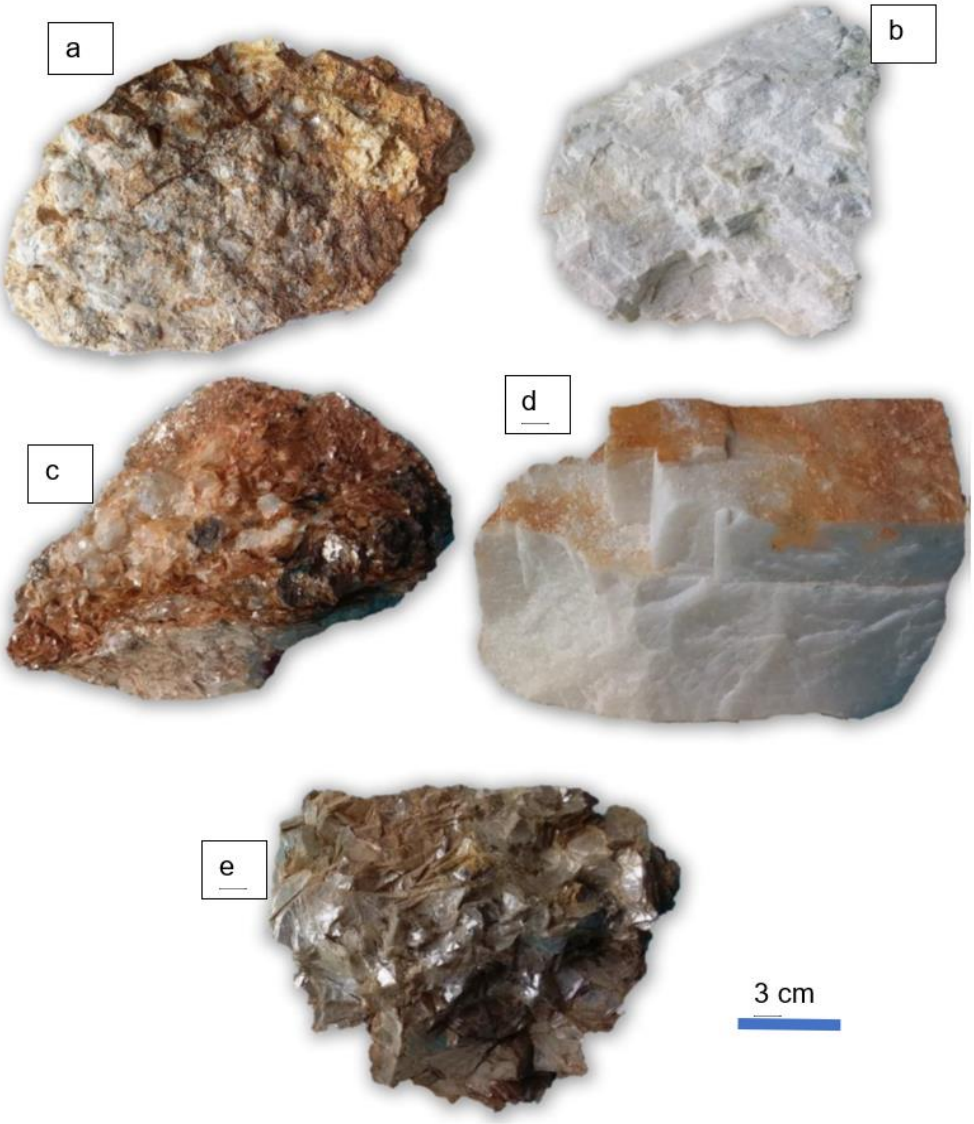

Plate 1: Characteristic features of hand specimens of Rod El-Biram pegmatites a) Brick-red K-feldspar, intermediate zone; b) Microcline in the intermediate zone; c) Quartz and muscovite in intermediate zone; d) Milky quartz, core zone; e) Isolated mica flakes, core zone.

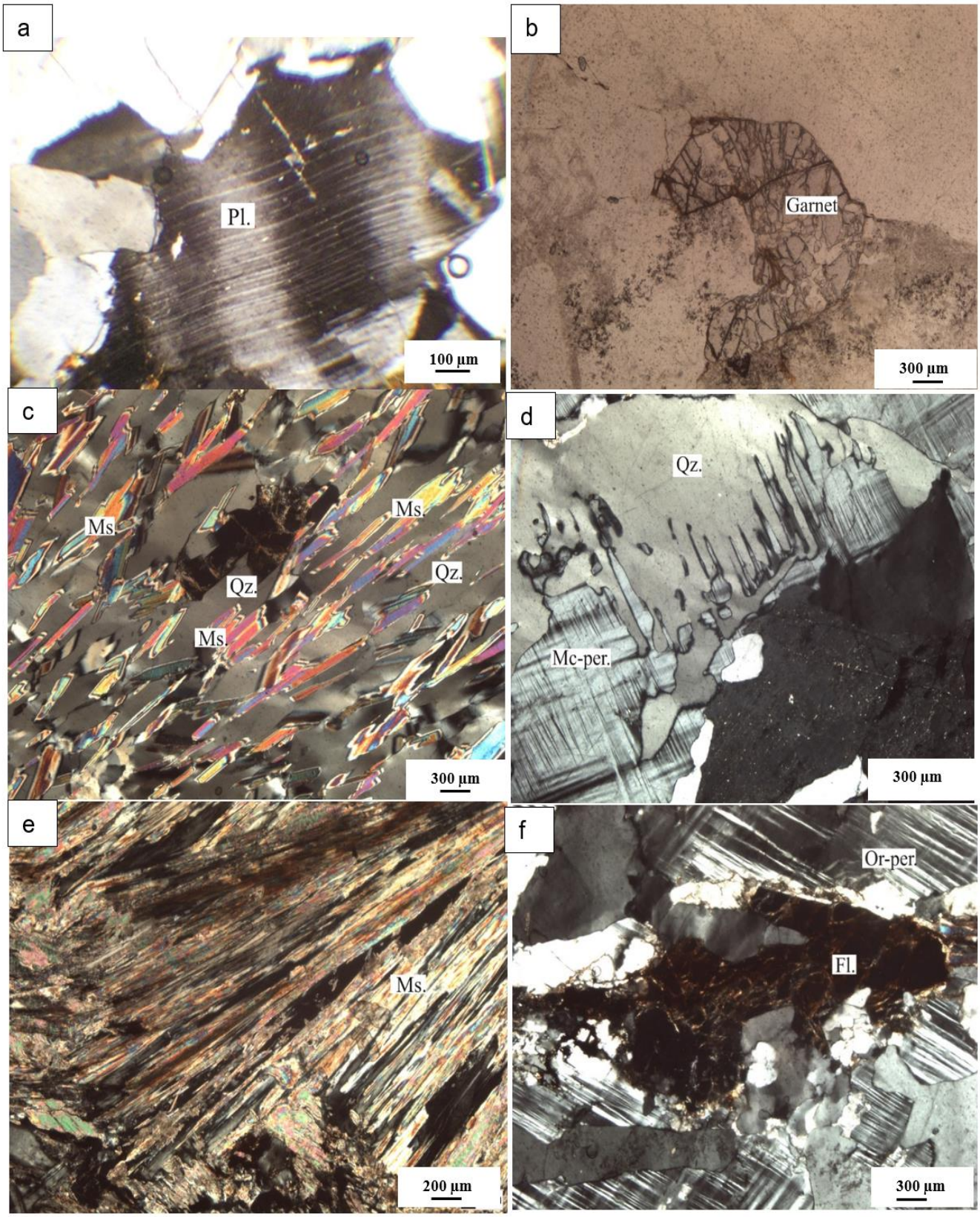

Fig.3: Microphotographs showing a) microfolded and cracked plagioclase in alkali-feldspar granites, *CN*, b) Subhedral garnet crystals in alkali-feldspar granites, *PPL*, c) Quartz (Qz) and muscovite (Ms), forming greisenized pockets along contact between alkali-feldspar granites and wall zone, *CN*, d) Flame type microcline perthite (Mc-Per) in intermediate zone, *CN,* e) variolitic shape muscovite (Ms) in intermediate zone *CN,* and f) isotropic flourite grains in intermediate zone, *CN*.

5. Heavy minerals

The separated heavy minerals include garnet [almandine $Fe^{2+}{}_3Al_2(SiO_4)_3$ and spessartine $[Mn^{2+}{}_3Al_2(SiO_4)_3]$, which exhibit different colors ranging from pale pink and orange to dark brown with vitreous luster. Almandine rose and is restricted with magnetite in 0.2 ampere fractions (Fig.4a), while spessartine is orange to dark brown euhedral crystals (Fig.4b) within 0.5 ampere fraction. Zircon [$ZrSiO_4$] occurs as euhedral to subhedral crystals. Elongation ratios range between 1.2 and 5, suggesting a magmatic origin of zircon (Pupin, 1980). Few varieties appear clear, while dominant crystals possess several inclusions of different shapes and sizes. Zircon shows metamictization due to due to the effect of radiation emitted from the enclosed uranium and thorium elements. Rutile [TiO_2] is commonly prismatic, elongated, and tabular in shape (Fig.4c). It has faint red grading into brownish red and black colors. Fluorite [CaF_2] normally occurs in very small sub-angular to sub-rounded grains, with characteristic green and violet colors. It is sometimes stained with iron oxyhydroxides (Fig.4d).

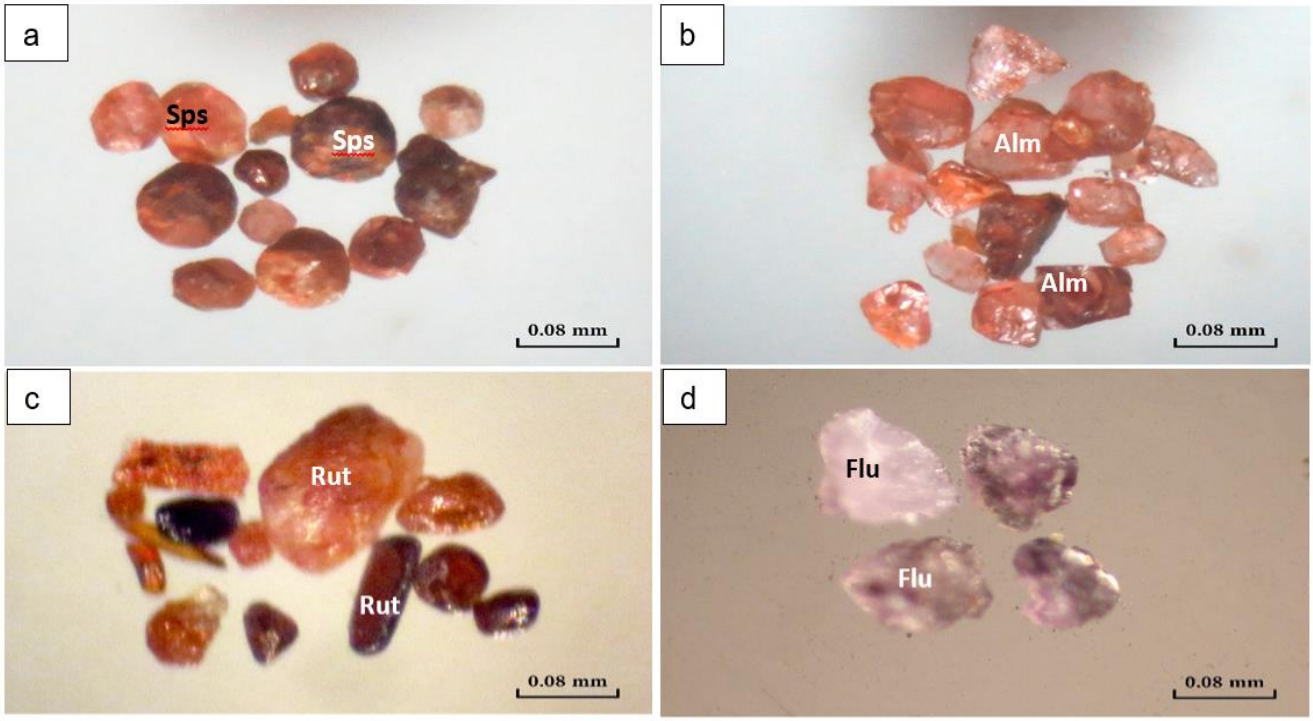

Fig. 4: Photomicrographs showing**,** a) spessartine garnet grains (Sps) stained with iron oxides, within 0.5 ampere fraction, b) almandine garnet grains (Alm) stained with iron oxides, within magnetite fraction, c) subhedral to anhedral rutile grains (Rut) with variable colors ranging from faint red to brownish red and black, within 1.0 ampere magnetic fraction and d) fluorite grains (Flu) with characteristic violet color, within 1.0 ampere nonmagnetic fraction.

6. Fluid inclusion

Fluid inclusions study is one of valuable tools in the understanding of late-magmatic and hydrothermal processes in the rocks. The present work includes the genetic and non-genetic description of fluid inclusions as well as phase transition (i.e., microthermometry). The latter represents the main aim of the fluid inclusions study.

Fluid inclusion study is one of valuable tools in the understanding of late-magmatic and hydrothermal processes (Abd El Monsef et al, 2023). Fluid inclusions can provide indispensable information about the environments and geologic processes in which the minerals were formed, particularly the composition, temperature, and pressure of the geofluids (Hollister & Crawford, 1981). Primary fluid inclusions are formed during, and as a direct result of growth of the surrounding host crystal. If a crystal fractures after it has been formed, some fluid may enter the fracture and become trapped as secondary fluid inclusions as the fracture heals. Thus, secondary inclusions are trapped after crystal growth is complete. If fracturing occurs during growth of the crystal, pseudo-secondary fluid inclusions may be trapped during continued crystal growth. Such inclusions are sometimes referred to as primary-secondary inclusions. Petrographically, the occurrence of pseudo-secondary inclusions is similar to secondary inclusions, but the latter are followed by additional crystal growth. Goldstein & Reynolds (1994) and Goldstein (2003) introduced the concept of the fluid Inclusion Assemblage (FIA) to describe a group of fluid inclusions that were all trapped at the same time.

6.1. Fluid inclusion petrography

Fluid inclusions investigated in Rod El-Biram pegmatites are represented mainly by one type distributed along lines and fluid inclusion planes as secondary inclusions. Based on the composition, these inclusions categorized to two subtypes 1a and 1b. Both subtypes occur in the same region (Fig.5a).

a) Subtype 1a, is represented by vapor rich H_2O-CO_2 inclusions (Fig. 5b) with CO_2 volume varies from 0.6 to 0.9 of the total volume of the inclusions. These inclusions are characterized by triangular, elongated, and oval shapes, and size varies from 10 - 20 um.

b) Subtype 1b, is two phases (L-V) with vapor phase representing up to 0.3 to 0.4 of the total volume of inclusions (Fig.5c). The shape is subangular and subrounded and the size is smaller (from 10 up to 15 um) relative to subtype 1a.

Mono-phase (L) and mono-phase (V) coexist with subtype1a and 1b within the same secondary lines or planes (Fig.5d).

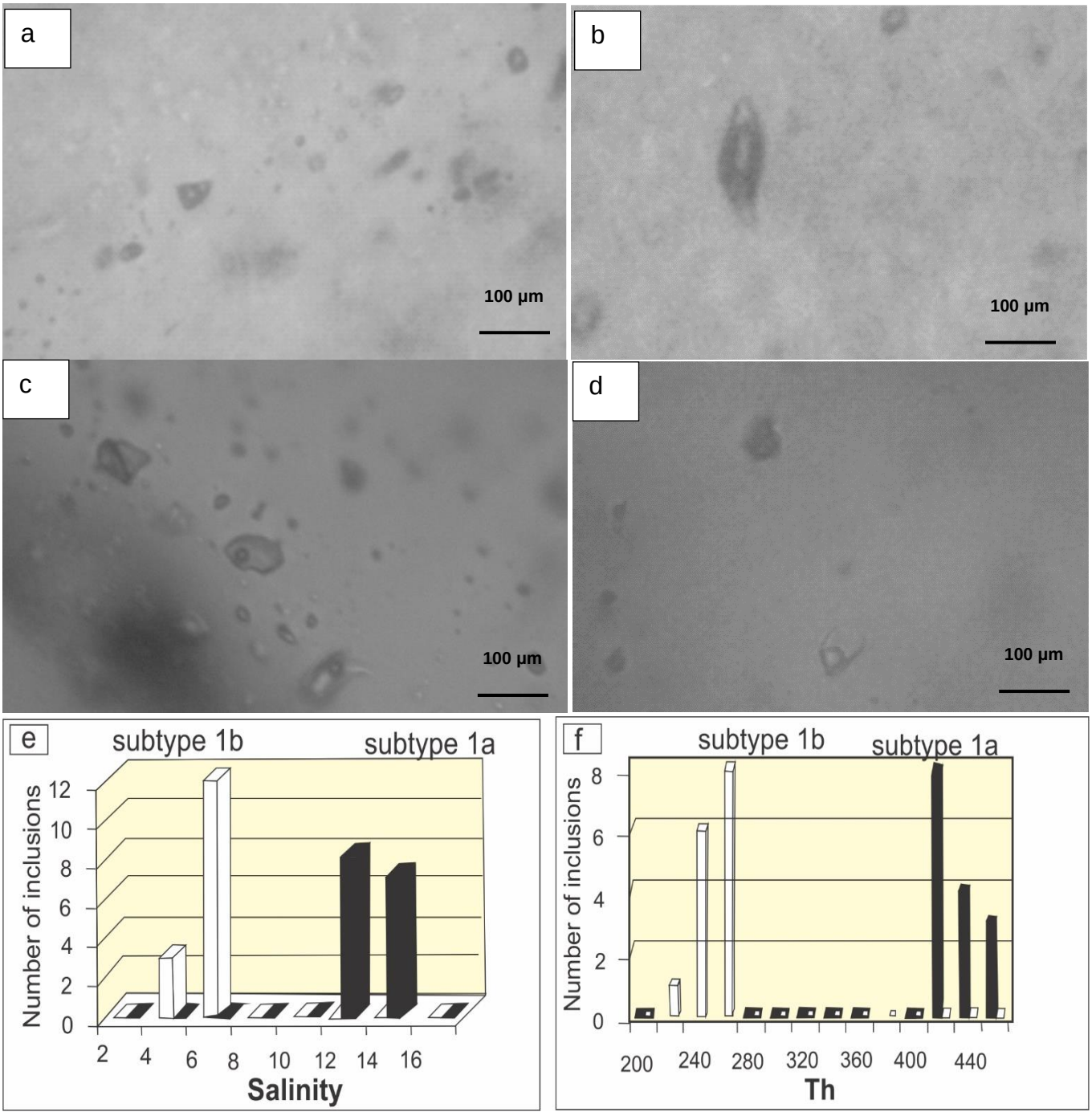

Fig.5: Graphs showing, a) coexisting of subtype 1a and 1b within the same region; b) Subtype 1a vapor rich inclusions; c) Primary two-phase aqueous inclusions; d) primary two-phase aqueous inclusions (type 1); e) The microthermometric salinity- frequency distribution of the inclusion; f) The homogenization temperature (Th)- frequency distribution of the inclusion in the studied pegmatites.

6.2 Microthermometric results

Microthermometric results are given in (Table 1), and (Fig.6e & f).

a) H_2O-CO_2 three phase inclusions

The melting of CO_2 (Tm_{CO2}) was measured at temperature between -55.8 °C to -57 °C, indicating pure CO_2-phase in the fluid system. Clathrate melt ($Tm_{clath.}$) estimated at temperatures between 2 °C and 3.4 °C, corresponding to salinity range from 11.43 to 13.26 wt. % NaCl eq. (Fig. 6e), with maximum peaks at 12wt. % NaCl eq. (Collins, 1979; Diamond, 1992). All CO_2 liquid and vapor phase homogenized to vapor at temperatures between 26 °C and 28 °C, corresponding to CO_2-densities estimated between 0.256 and 0.289 g/cm^3.

Bulk homogenization is achieved at temperatures between 420 °C and 450 °C, with the majority at 420°C (Fig. 6f).

b) Two-phase aqueous inclusions

The eutectic (Te) was achieved at few inclusions at temperature up to -51 °C, indicating the presence of CaCl. In addition to NaCl dissolved in the aqueous phase. The temperature of final melting of ice (Tm_{ice}) measured at temperatures between -2 °C and -3 °C, corresponds to low salinity between 3.39 and 4.96 wt.% NaCl eq. (Bodnar, 1993), with the majority at 5 wt.% NaCl eq. The bulk homogenization is achieved at temperatures between 220 °C and 260 °C, with maximum peak at 250 °C. Dissolution of daughter crystals achieved in few inclusions at temperature 430 °C, corresponding to high salinity 51 wt. % NaCl eq. (Table 1).

Table 1: Microthermometric results of the studied pegmatites.

Inclusion type and parameters	Measurements
Two- phase (L+V) aqueous inclusions	
Th_{tot} (°C):	220 °C to 260 °C
T_{mice}:	-3 °C to -2°C
Salinity in wt% NaCl eq.:	3.55 °C to 4.96 °C
T_e (°C):	-51°C
Distribution:	S

L (liquid), V (Vapor), S (Solid), Th_{tot} (temperature of homogenization), T_{mic} (final melting of ice),Th_e (eutectic temperature) and S (secondary).

7. Mineral chemistry of muscovite and K-feldspar

Muscovites in Wadi Rod El-Biram could be separated easily and analyzed because they occur as large flakes or fan-shape aggregates. The chemistry of separated muscovite and K-feldspar is shown in table (2). Primary muscovites have higher Ti, Na, Al and lower Mg and Si than secondary one. Ti content is preferable indicator for primary muscovite rather than Na, Al and Si because the former is not affected by secondary processes (Zen, 1988; Speer, 1984). Monier et al. (1984) distinguished three genetic types of muscovite: magmatic, late- to post-magmatic and hydrothermal muscovite using the $Fe_2O_3^t$ - TiO_2-MgO ternary diagram. Rod El-Biram muscovites fall within magmatic muscovite field (Fig.6a). The alkali-feldspar has low anorthite contents (0.04%). Furthermore, the plots of feldspar analyses on Ab-An-Or diagram (Smith & Brown, 1988), show that K-feldspar in the pegmatite of Rod El-Biram have perthite and perthite-orthoclase composition (Fig.6b).

Table 2: Chemistry and structural formula of muscovite and K-feldspar from Rod El-Biram pegmatites.

Locality	Muscovite		K-feldspar	
Sample	B11	B28	B8	B9b
SiO_2	47.80	47.80	73.74	66.70
TiO_2	0.12	0.01	0.01	0.01
Al_2O_3	35.30	36.20	14.37	20.02
Fe_2O_3	2.20	1.67	0.06	0.02
MnO	0.01	0.01	0.01	0.01
MgO	0.01	0.01	0.01	0.01
CaO	0.01	0.01	0.01	0.01
Na_2O	0.04	0.01	1.97	0.01
K_2O	9.39	9.39	9.23	11.70
P_2O_5	0.01	0.01	0.01	0.01
Cl	0.01	0.01	--	--
H_2O*	4.52	4.55	---	----
Total	99.41	99.68	99.42	98.5
Structural formula based on 12 oxygen atoms			Structural formula based on 8 oxygen atoms	
Si	6.33	6.29	0.01	0.01
Al ^{iv}	1.67	1.71	2.97	2.71
Al ^{vi}	3.84	3.91	0.77	1.08
Ti	0.01	0.00	0.000	0.000
Fe	0.24	0.18	0.005	0.002
Mn	0.00	0.00	0.001	0.001
Mg	0.00	0.00	0.001	0.001
Ca	0.00	0.00	0.001	0.001
Na	0.01	0.00	0.32	0.00
K	1.59	1.58	1.49	1.90
P	0.0003	0.0003	0.0003	0.0003
OH*	4.00	4.00	----	----
Cl	0.00	0.00	---	---
TOTAL	17.70	17.68	5.55	5.70
Y $_{total}$	4.10	4.10	--	---
X $_{total}$	1.60	1.58	---	
Al total	5.51	5.62	---	----
Fe/Fe+Mg	0.99	0.99	---	---
Or	--	---	82.37	99.87
Ab			17.58	0.09
An			0.04	0.04

*H_2O calculation **(**after Tindle & Webb, 1990**)**

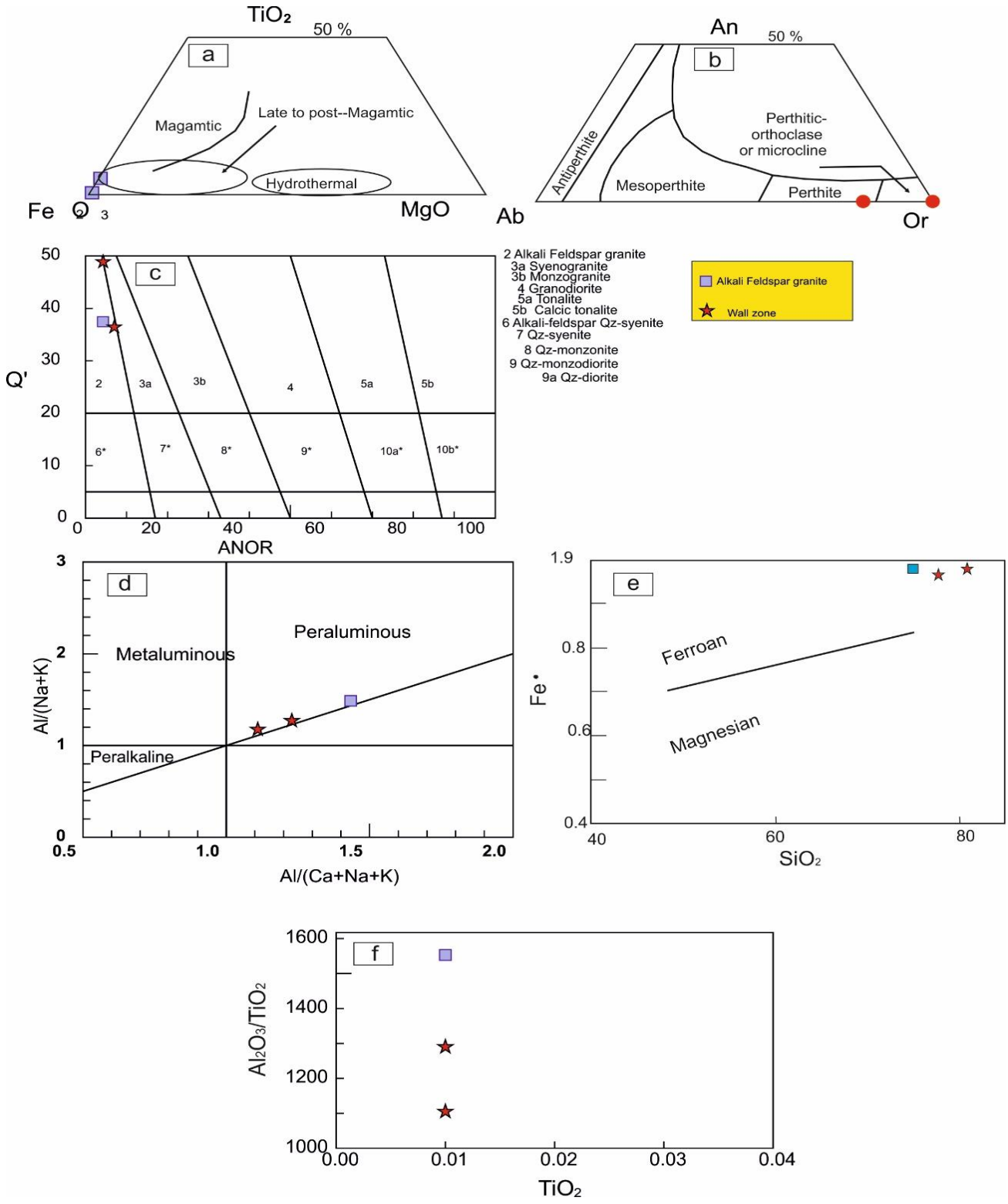

Fig. 6: a) FeO_t- TiO_2-MgO ternary diagram (Monier et al., 1984) for the studied muscovite; b) Ab-An-Or diagram of Smith & Brown (1988) for the studied K-feldspar; c) Q' and ANOR diagram for the classification of the plutonic rock (Streckeisen & Le Maitre, 1979); d) Molar A/CNK vs. A/NK diagram of Shand (1947); e) SiO_2- Fe * (FeO_{tot} / FeO_{tot}+ MgO) diagram (Frost & Frost, 2008) and f) TiO_2 versus Al_2O_3/TiO_2 diagram.

8. Geochemical characteristics

By comparing the chemistry of the hosted alkali-feldspar granites with intermediate and wall zones, the following results are shown (Table 3). The silica and Na_2O contents in Wadi Rod El-Biram pegmatites also increases from intermediate zone through associated granites to border zone and vice versa for K_2O content (Table 3). In contrast, the concentration of Alumina increases from intermediate zone through wall zone to granitic rocks. No notable variation was observed in other major oxides. The classification of the plutonic rocks using the Q' versus ANOR diagram (Streckeisen & Le Maitre, 1979) reveals that the granite and wall zone samples of Wadi Rod El-Biram fall within the field of alkali feldspar granite (Fig.6c). According to A/CNK vs. A/NK diagram of Shand (1947) the alkali-feldspar granite and wall zone samples have strong peraluminous characters (Al/ (Ca + Na + K)> 1.1; Fig.6d), so they belong to S-type. The plots of SiO_2- Fe * (FeO_{tot} / FeO_{tot}+ MgO) diagram (Frost & Frost, 2008) indicate that, the magmatic source of alkali-feldspar granite and wall zone samples are ferroan (Fig. 6e).

The trend shown in TiO_2 versus Al_2O_3/TiO_2 diagram (Fig. 6f) is not compatible with the fractional crystallization trend (Garcia et al. 1994), which indicates that the studied pegmatite has a different source from rather than granitic melt. The crystallization temperatures were calculated using Al-Ti thermometer ($T_{Al\text{-}Ti}$ °C) according to (Jung & Pfänder, 2007) equation (Table 2). The temperature values estimated for pegmatite samples fluctuate from 481.5°C to 498.5°C.

9. Suitability for ceramic industry

Alkali-feldspars from pegmatites are widely used in ceramic and glass industries as a flux. On the other hand, the Ca-rich plagioclase feldspars are not used as flux, because they melt at high temperatures, and they are usually contaminated by iron and titanium. However, they are used for special types of ceramics. The ceramic industry depends on the knowledge of raw materials, physical and chemical properties of the minerals and their aggregates present in ceramic raw materials and their behavior during manufactories.

9.1 Chemical composition of K-feldspar

The comparison between the chemical analyses results of alkali-feldspar samples collected from the three areas with the standard chemical specifications for feldspars used in ceramic industry is given in table (3).

K-feldspars have wide variation of SiO_2 which range from (73.74 wt.% to 66.70 wt.%), TiO_2 (0.01 wt. %), Al_2O_3 range from (14.37 wt. % to 20.02 wt. %), Fe_2O_3 range from (0.06 wt. % to 0.02 wt. %), MnO (0.01 wt.%), MgO (0.01 wt. %), CaO (0.01 wt. %), Na_2O range from (1.97 wt. % to 0.01 wt. %), K_2O range from (9.23 wt. % to 11.70 wt. %) and P_2O_5 (0.01 wt. %). Comparing these results with the standard chemical specifications for feldspars used in ceramic industry indicates a good similarity. Furthermore, the quality of tiles is controlled by three factors: shrinkage, water absorption and bending strength according to international standard limit (Konta, 1980) after the system of firing.

Table 3: Major element concentration (wt %) of alkali-feldspar granites and wall and intermediate zones of Wadi Rod El-Biram pegmatites with the standard limits used for ceramic industry raw material by Ceramica Cleopatra Company (Personal communication).

Locality	Wadi Rod El-Biram				Standard limits	
Rock type	Alkali- feldspar granites Av. (3) *	Wall zone		Intermediate zone	From	To
Oxides		B13	B21	B8		
SiO_2	74.90	80.85	77.70	73.74	68	78max.
TiO_2	0.01	0.01	0.01	0.01	0	0.1
Al_2O_3	15.53	11.05	12.90	14.37	11	16
Fe_2O_3	0.52	0.51	0.30	0.06	0	2max.
MnO	0.01	0.01	0.01	0.01	0	0.5
MgO	0.01	0.01	0.01	0.01	0	1max.
CaO	0.21	0.16	0.35	0.01	0	1max.
Na_2O	3.89	3.48	4.21	1.97	1	4
K_2O	3.74	2.75	3.75	9.23	4%nim.	over
P_2O_5	0.01	0.01	0.01	0.01		
Cl	0.01	0.01	0.01	0.01		
L.O.I	0.94	0.89	0.52	0.34		
Total	99.77	99.75	99.78	99.77		
$T_{Al\text{-}Ti}$ °C**	-	498.5	481.5	-		

*****Average of alkali-feldspar granites from El-Shibiny (2016).

**$T_{Al\text{-}Ti}$ °C is crystallization temperature obtained by calibrated Al-Ti thermometer (Jung & Pfänder, 2007).

9.2 Physical testing

There are many tests that were done for K-feldspar to adapt the quality of feldspars for ceramic industry. These tests include shrinkage, water absorption and bending strength, surface hardness and resistance to thermal shocks. These tests were applied on a biscuit sample. The results of measuring the three parameters (i.e. binding strength, shrinkage and water absorption) indicate that the green biscuit ceramic samples that prepared from Wadi Rod El-Biram pegmatite bodies are suitable for of floor ceramic tiles industry rather than wall tiles (Table 4).

Table 4: The ceramic physical parameters for the tested samples from the studied pegmatites compared with standard limits after (Knota, 1980).

Sample no.	G15 (Av. 3)	G18 (Av. 3)	Standard limits	
			Floor	Wall
Shrinkage %	5.2%	6.3 %	<3%	14-17%
Bending stress	34.5	41	>27.5 newton /cm^2	>17 newton /cm^2
Water absorption %	0.62 %	0.25 %	0-3%	5-6.5%

10. Concluding remarks

Rod El-Biram pegmatites outcrop in the Central Eastern Desert at latitude 25º 8` 30`` and 25º 11` 00`` N and longitude 34º 00` 00`` and 34º 10` 00`` E. Rod El-Biram pegmatite bodies invade both alkali-feldspar granites and ophiolitic serpentinites. The pegmatite bodies are made mainly of muscovite-bearing type and occur as round and/or elongated masses. The zoned bodies consist of three successive zones, the outer zone (wall zone) is mainly composed of albite and muscovite. Greisenized pockets are recorded along contact between alkali-feldspar granites and the wall zone of pegmatite bodies. The intermediate zone is composed mainly of blocky K-feldspar. This zone contains subordinate amounts of quartz and muscovite. The inner zone (core zone), which consists of milky quartz, forms an amoeboid shape. This zone sometimes encloses isolated flakes and/or nests of muscovite. The heavy minerals are represented by garnet (almandine and spessartine), fluorite, zircon, and rutile. The presence of garnet in granites and pegmatites derived either by garnet crystallization with muscovite as an alternative to biotite from volatile enriched melt (Gindy, 1965) or by assimilation from country rocks (Brammall & Harwood, 1932). Rutile formed as a result of the partial alteration of ilmenite, indicating a post-magmatic alteration process.

Fluid inclusions investigated in Rod El-Biram Pegmatites are represented mainly by one type distributed along lines and fluid inclusion planes as secondary inclusions. Based on the composition, these inclusions categorized to two subtypes: a) Subtype 1a, is represented by vapor rich H_2O-CO_2 inclusions (Fig. 5b) with CO_2 volume varies from 0.6 to 0.9 b) Subtype and 1b) is two phases (L-V) with vapor phase (Fig. 5c). In the H_2O-CO_2 three phase inclusions, the melting of CO_2 (Tm_{CO2}) was measured at temperature between -55.8 ºC to -57 ºC, indicating pure CO_2-phase in the fluid system. Clathrate melt ($Tm_{clath.}$) estimated at temperatures between 2 ºC and 3.4 ºC, corresponding to salinity range from 11.43 to 13.26 wt. % NaCl eq. (Fig. 6e), with maximum peaks at 12wt. % NaCl eq. (Collins, 1979; Diamond, 1992). The bulk homogenization is achieved at temperatures between 420 ºC and 450 ºC, with the majority at 420 ºC (Fig. 6f). In the two-phase aqueous inclusions, the eutectic (Te) was achieved at few inclusions at temperature up to -51ºC, indicating the presence of CaCl. In addition to NaCl dissolved in the aqueous phase. The temperature of final melting of ice (Tm_{ice}) measured at temperatures between -2 ºC and -3ºC, corresponds to low salinity between 3.39 and 4.96 wt.% NaCl eq. (Bodnar, 1993), with the majority at 5 wt.% NaCl eq. The bulk homogenization is achieved at temperatures between 220 ºC and 260 ºC, with maximum peak at 250 ºC. The dissolution of daughter crystals achieved in few inclusions at temperature 430 ºC, corresponding to high salinity 51 wt. % NaCl eq. (Table 1).

Rod El-Biram muscovites belong to primary, magmatic muscovite. The studied wall zone samples have alkali-feldspar granite composition (Fig. 6c). In addition, the magma type of both the country alkali-feldspar granite and the wall zone of the studied pegmatite body are strongly peraluminous (i.e. S-type) and ferroan (Fig. 6 d & e). The trend of the granitic rock and associated pegmatites in Rod El-Biram is not compatible with the fractional crystallization trend from alkali-feldspar granite to pegmatite (Fig.6f), so these pegmatites have different sources rather than the granitic melt. The calculated crystallization temperatures of the wall zone of pegmatite body obtained by calibrated Al-Ti thermometer (Jung & Pfänder 2007) range between 481.5-408.5 °C (Table 3). Muscovite, apatite, and garnet in Road El-Biram muscovite pegmatite represent source for Li, Light Rare-Earth Elements (REE), Nb, Ta, U respectively. According to Cerny (1991) muscovite pegmatite have no relation to the granites (i.e. anatectic bodies) and related to Barrovian amphibolite facies metamorphic environment. By comparing the chemical composition of K-feldspar from Rod El-Biram pegmatites body with the standard chemical specifications and physical testing on the green biscuits with standard chemical composition and physical parameters range for the raw material used in ceramic industry confirms the suitability of the feldspars from the area for ceramic industry in floor rather than wall ceramic tiles (Tables 3 & 4).

References

Abd El Monsef M, Sami M, Toksoy-Köksal F, et al. (2023): Role of Magmatism and Related-Exsolved Fluids during Ta-Nb-Sn Concentration in the Central Eastern Desert of Egypt: Evidence from Mineral Chemistry and Fluid Inclusions. J. Earth Scie 34 (3): 674-689, https://doi.org/10.1007/s12583-022-1778-y

Abu Elatta SA (2019): Geology, mineralogy and mineral chemistry of the NYF-type pegmatites at the Gabal El Faliq area, South Eastern Desert, Egypt. J Earth System Scie 128-156, https://doi.org/10.1007/s12040-019-1169-7

Bowers, TS, Helgeson HC (1983): Calculation of the thermodynamic and geochemical consequences of nonideal mixing in the system H2O-CO2-NaCl on phase-relations in geologic systems - Metamorphic equilibria at high-pressures and temperatures. Am Mineral 68 (11-12): 1059-1075.

Brammall, A., Harwood H.F. (1932): The Dartmoor granites: their genetic relationships. Quart. J Geol Soc Lond 88:171-237.

Brown, P.E. (1989): FLINCOR: A Microcomputer Program for the Reduction and Investigation of Fluid Inclusion Data. Am Mineral 74: 1390-1393.

Cameron EN, Jahns RH, MeNair AH, Page LR (1949): Internal structure of granitic pegmatites: Econ Geol Mono 2:115p.

Černy P (1982): Petrogenesis of granitic pegmatites. In: Černy P (ed.): Granite pegmatites in science and industry Mineral Assoc. Canada Short course 8: 461p.

Černy P (1991): Rare-element granitic pegmatites. Part 1: Anatomy and internal evolution of pegmatite deposits. Part 2: Regional to global environments and petrogenesis. Geosci Canada 18: 49- 81.

Černy P, Ercit TS (2005): Classification of granitic pegmatites revisited. Can Mineral 43: 2005-2026.

Černý P, London D, Novak M (2012): Granitic pegmatites as reflections of their sources. Elements 8: 289-294, https://doi.org/10.2113/gselements.8.4.289

Collins PLF (1979): Gas hydrates in CO_2-bearing fluid inclusions and the use of freezing data for estimation of salinity. Econ Geol 74: 1435-1444, https://doi.org/10.2113/gsecongeo.74.6.1435

Dardier AM (1997): Geology, petrology, and radioactivity of some granitic masses in the area of Gabal Abu Diab, Eastern Desert, Egypt. PhD Thesis, Ain Shams Univ., Egypt. 179 p.

Diamond LW (1992): Stability of CO_2-clathrate-hydrate + CO_2 liquid +CO_2 vapour + aqueous KCl-NaCl solutions: Experimental determination and application to salinity estimates of fluid inclusion. Geochim Cosmochim Acta 56: 273-280, https://doi.org/10.1016/0016-7037(92)90132-3

El-Nahas HA (1997): Geochemistry and mineralogy of some radioactive pegmatites, Abu Zawal area, Easten Desert, Egypt. MSc. Thesis, Faculty Science, Menofiya University, Egypt 140p.

El-Shibiny NH (2016): Contributions to the Geochemistry, Mineral chemistry and Genesis of Rod Ashab Pegmatite Zones, Central Eastern Desert, Egypt. Ann Geol Surv Egypt XXXIII, 147-172.

Fawzy, M. M., Mahdy NM, Sami M (2020): Mineralogical characterization and physical upgrading of radioactive and rare metal minerals from Wadi Al-Baroud granitic pegmatite at the Central Eastern Desert of Egypt. Arab J Geosci 13 (11): 413, https://doi.org/10.1007/s12517-020-05381-z

Frost BR, Frost CD (2008): A geochemical classification for feldspathic igneous rocks. J Petrol 49: 1955–1969, https://doi.org/10.1093/petrology/egn054

Garcia D, Fonteilles M, Moutte J (1994): Sedimentary fractionation between Al, Ti, and Zr and the genesis of strongly peraluminous granites. J Geol 102: 411- 422, https://doi.org/10.1086/629683

Gindy AR (1956): A- Biotite schlieren in sonie intrusive granités from the Eastern Desert of Egypt and Donegal, Eire. Bull Inst Désert Égypte 6: 159.

Ginsburg AI (1984): The geological condition of the location and the formation of granitic pegmatites: 27th IGC proceedings 15: 245-260.

Goldstein RH (2003): Petrographic analysis of fluid inclusions. In: Samson I, Anderson A, Marshall D (eds.): Fluid Inclusions: Analysis and Interpretation. Mineralogical Association of Canada Short Course 32: 9-53.

Goldstein RH, Reynolds TJ (1994): Systematics of fluid inclusions in diagenetic minerals: Society for Sedimentary Geology Short Course 31:199 pp.

Hollister LS, Crawford ML (1981): Fluid Inclusions-Applications in Petrology; Mineralogical Association of Canada Publications: Québec, QC, Canada 6: 304 p.

Ibrahim, ME, Saleh GM, Dawood MI, Kamar MS, Saleh SM, Mahmoud MA, El- Tohamy AM (2017): Rare metals mineralization in pegmatite at Abu Rusheid Area, South Eastern Desert, Egypt. Inter J Min Scie 3 (1): 44-63, http://dx.doi.org/10.20431/2454-9460.0301004

Jung S, Pfänder JA (2007): Source composition and melting temperature of orogenic granitoids: constraints from CaO/Na_2O, Al_2O_3/TiO_2 and accessory mineral saturation thermometry. Euro J Mineral 19 (6): 859-870, https://doi.org/10.1127/0935-1221/2007/0019-1774

Khaleal FM, Saleh GM, Lasheen ESR, Alzahrani AM and Kamh SZ (2022): Exploration and Petrogenesis of Corundum-Bearing Pegmatites: A Case Study in Migif-Hafafit Area, Egypt. Front. Earth Sci. 10, 869- 828, https://doi.org/10.3389/feart.2022.869828

Konta J (1980): Properties of Ceramic Raw Materials" Ceramic Monographs- Handbook of Ceramics. Verlag Schimd GmbH, Freiburg.

Martin RF, De Vito C (2005): The patterns of enrichment in felsic pegmatites ultimately depend on tectonic setting. Can Mineral 43: 2027-2048.

Monier G, Mergoil-Daniel J, Labernardière H (1984): Générations successives de muscoviotes et feldspaths potassiques dans les leucogranite du massif de Millevaches (Massif Central Francais). Mineralogical Association of Canada Short Course, de Mineralogie 107: 55-68.

Moustafa MI, Ragab AA, Ibrahim ME (2002): Mineralogy and petrogenesis of muscovite in wall zone, Rod El-Biram pegmatite, Central Eastern Desert, Egypt. 6th Inter Conf Geol of the Arab World, Cairo University, 67-80.

Müller A, Romer RL, Pedersen R-B (2017): The Sveconorwegian pegmatite province–thousands of pegmatites without parental granites. Can Mineral 55 (2): 283-315

Omar SA (1995): Geological and geochemical features of the radioactive occurrences south G. Um Anab granitic masses, Eastern Desert, Egypt: MSc. Thesis, Cairo University, 164p.

Poty B, Leroy J, Jakimowicz L (1976): Un nouvel appareil pour la mesure des temperatures sous le microscope: l`Installation de microthermometrie Chaixmeca. Bulletin de la Societe francaise de Mineralogie et Cristallographie 99: 182-186.

Pupin, J.-P., 1980. Zircon and granite petrology. Contrb Mineral Petrol 110: 463-472, https://doi.org/10.1007/BF00381441

Rashwan AA (1991): Petrography, geochemistry and petrogenesis of the Migif-Hafafit gneisses at Hafafit mine area, South Eastem Desert, Egypt. Sci Ser Intem Barea 5: Forschangszentran Julich GmbH, 359 p.

Raslan MF, Ali MA (2011): Mineralogy and mineral chemistry of rare-metal pegmatites at Abu Rusheid granitic gneisses, South Eastern Desert, Egypt. Geologija 54/2: 205-222, http://dx.doi.org/10.5474/geologija.2011.016

Raslan MF, Ali MA, El Feky, MG (2010b): Mineralogy and radioactivity of pegmatites from South Wadi Khuda area, Eastern Desert, Egypt. Chin J Geochem 29: 34-354, https://doi.org/10.1007/s11631-010-0466-2

Raslan MF, El-Shall HE, Omar SA, Daher AM (2010a): Mineralogy of polymetallic mineralized pegmatite of Ras Baroud granite, Central Eastern Desert, Egypt. J Mineral Petrol Sci 105 (3):123–134. https://doi.org/10.2465/jmps.090201

Rudenko SA, Romanov VA, Morakhovskiy VN, Tarasov EB, Galkin GA, Dorokhin VK (1975): Conditions of formation and controls of distribution of muscovite objects of the North-Baikal muscovite province, and some general problems of pegmatite consolidation: in Muscovite Pegmatites of the USSR, Nauka publishing house, Leningrad: 74-182 (in Russian).

Saleh GM (2007): Rare metal-bearing pegmatites from the south-eastern desert of Egypt: Geology, geochemical characteristics, and petrogenesis. Chin J Geochem 26 (1): https://doi.org/10.1007/s11631-007-0008-8

Saleh GM, Afify AM, Emad BM, Dawoud MI, Shahin HA, Khaleal FM (2019): Mineralogical and geochemical characterization of radioactive minerals and rare earth elements in granitic pegmatites at G. El Fereyid, South Eastern Desert, Egypt. J Afr Earth Sci 160: 103651, https://doi.org/10.1016/j.jafrearsci.2019.103651

Shalaby MH, Salman AB, El Kammar AM, Mahdy AI (1999): Uranium mineralization in the Hammamat sediments of the Gattar area, Northeasten Desert, Egypt. 4th Inter Conf Geochem Alexandria University, Egypt, 101-121.

Shand, S.J. (1947): Eruptive rocks, their genesis, composition, classification, and their relation to ore deposits, with a chapter on meteorites, 3rd ed. Thomas Murphy, London, 488 p.

Smith, J. V and Brown, W.L. (1988): Spectroscopy—IR, Raman, NMR, NQR, PR, NGR (Mössbauer), XAS, EXAFS, ESCA, XPS, Feldspar Minerals. Springer, 44–267.

Speer, J.A. (1984): Micas in igneous rocks. In: Bailey SW (ed.), Micas, Reviews in Mineralogy 13: Mineralogical Society of America, Washington DC, 299-356, https://doi.org/10.1515/9781501508820-013

Streckeisen A, Le Maitre RW (1979): A chemical approximation to the modal QAPF classification of the igneous rocks. Neues Jahrb. Mineral., Abh. 136, 169–206.

Tindle AG, Webb PC (1990): Estimation of lithium contents in trioctahedral micas using microprobe data; application to micas from granitic rocks. Europ J Mineral 2(5): 595-610. http://eurjmin.geoscienceworld.org/cgi/content/abs

Wise MA (1999): Characterization and classification of NYF-type pegmatites. Can Mineral 37: 802-803.

Zen E-AN (1988): Phase relations of peraluminous granitic rocks and their petrogenetic implications. Annual Review in Earth Planet Sci 16: 21–51, https://doi.org/10.1146/annurev.ea.16.050188.00032

Zhang Y, Frantz D (1987): Determination of the homogenization temperatures and densities of supercritical fluids in the system NaClKClCaCl2H2O using synthetic fluid inclusions. Chemical Geology, 64, 335-350, https://doi.org/10.1016/0009-2541(87)90012-X